Akt regulates centrosome migration and spindle orientation in the early *Drosophila melanogaster* embryo

Graham J. Buttrick,[1] Luke M.A. Beaumont,[2,3] Jessica Leitch,[3] Christopher Yau,[3] Julian R. Hughes,[1] and James G. Wakefield[1,3]

[1]Department of Zoology, University of Oxford, Oxford OX1 3PS, England, UK
[2]Department of Engineering, University of Oxford, Oxford OX1 3PJ, England, UK
[3]Life Sciences Interface Doctoral Training Centre, University of Oxford, Oxford OX1 3QD, England, UK

Correct positioning and morphology of the mitotic spindle is achieved through regulating the interaction between microtubules (MTs) and cortical actin. Here we find that, in the *Drosophila melanogaster* early embryo, reduced levels of the protein kinase Akt result in incomplete centrosome migration around cortical nuclei, bent mitotic spindles, and loss of nuclei into the interior of the embryo. We show that Akt is enriched at the embryonic cortex and is required for phosphorylation of the glycogen synthase kinase-3β homologue Zeste-white 3 kinase (Zw3) and for the cortical localizations of the adenomatosis polyposis coli (APC)–related protein APC2/E-APC and the MT + Tip protein EB1. We also show that reduced levels of Akt result in mislocalization of APC2 in postcellularized embryonic mitoses and misorientation of epithelial mitotic spindles. Together, our results suggest that Akt regulates a complex containing Zw3, Armadillo, APC2, and EB1 and that this complex has a role in stabilizing MT–cortex interactions, facilitating both centrosome separation and mitotic spindle orientation.

Introduction

Many cellular processes, including vesicle transport, cell polarization, centrosome separation, and cytokinesis rely on the coordinated organization of the F-actin and microtubule (MT) cytoskeletons (Goode et al., 2000; Siegrist and Doe, 2007). Both these cytoskeletal elements possess an intrinsic polarity and, as such, transmit positional information within the cell. In general, actin is enriched at the cell cortex, whereas MTs are nucleated predominantly by the centrosome that, during interphase, is juxtaposed with the nuclear envelope. Signals transmitted between the MTs and the actin filaments thus allow the cell to synchronize events occurring at the edge of the cell with processes taking place in the cell interior.

Drosophila melanogaster embryos provide an excellent system in which to study the interactions between cytoskeletal elements. The first 13 mitoses that constitute the syncytial blastoderm stage occur rapidly, synchronously, and within a common cytoplasm. During cycles 9 and 10, the nuclei and associated centrosomes migrate from the interior of the embryo to the cortex, where they are maintained by interactions between MTs and cortical F-actin (for review see Sullivan and Theurkauf, 1995). These centrosomes duplicate during telophase and nucleate at least two populations of MTs: those with plus ends that extend upwards to the actin-rich cell cortex and those that interdigitate between the sister centrosomes. The centrosomes progressively separate throughout the following interphase until, by nuclear envelope breakdown (NEB), the centrosomal pairs lie approximately opposite one another. Both experimental and mathematical evidence have shown that, although the major contributor to centrosome separation is a sliding of the antiparallel crosslinked MTs facilitated by opposing MT motor proteins, the actin cytoskeleton is also necessary for centrosomes to complete separation (Sharp et al., 2000; Stevenson et al., 2001; Cytrynbaum et al., 2003, 2005).

The coordination between the cytoskeletal elements that occurs in the *D. melanogaster* embryo is facilitated in part by regulating protein complexes that link the MT plus ends to actin filaments. One such complex includes the wingless signaling components Zeste-white 3 (Zw3; the *D. melanogaster* homologue of glycogen synthase kinase-3 [GSK-3]), Armadillo (Arm, the *D. melanogaster* homologue of β-catenin), and the adenomatous

Correspondence to J.G. Wakefield: james.wakefield@zoo.ox.ac.uk

Abbreviations used in this paper: APC, adenomatous polyposis coli; Arm, Armadillo; GSK-3, glycogen synthase kinase-3; MT, microtubule; NEB, nuclear envelope breakdown; PI3-K, phosphoinositide 3-kinase; Zw3, Zeste-white 3.

The online version of this paper contains supplemental material.

© The Rockefeller University Press $30.00
The Journal of Cell Biology, Vol. 180, No. 3, February 11, 2008 537–548
http://www.jcb.org/cgi/doi/10.1083/jcb.200705085

THE JOURNAL OF CELL BIOLOGY

Downloaded from www.jcb.org on February 15, 2008

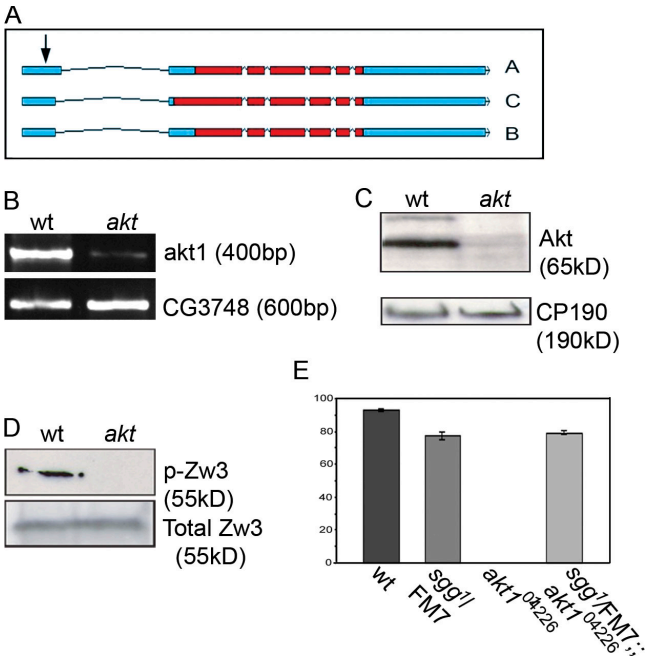

Figure 1. ***D. melanogaster* Akt regulates Zw3 during early embryonic development.** (A) Representation of the *akt* locus showing differential splicing of the three proposed isoforms (A, B, and C) and the site of insertion of the PZ *P* element (arrow). Coding regions are shown in red and untranslated regions are shown in blue (adapted from Flybase; http://www.flybase.indiana.org). (B) RT-PCR of a 400-bp region of the *akt* coding region from cDNA extracted from wild-type and *akt* mutant flies. (C) Western blot of 0–3-h embryo extracts probed with antibodies specific for Akt. CP190 is shown as a loading control. (D) Western blot of embryo extracts probed with an antibody specific for Zw3 phosphorylated on the consensus Akt phosphorylation site (Ser^{12}). (E) Histogram demonstrating the rescue of $akt1^{04426}$ female sterility through the introduction of one copy of sgg^{1}. Error bars indicate the SEM.

polyposis coli (APC)–related protein APC2/E-APC (McCartney et al., 2001; Cliffe et al., 2004). Mutations in the gene encoding APC2 lead to loss of syncytial nuclei into the interior of the embryo before cellularization (a process termed nuclear fallout). In addition, both APC2 and Arm have been shown to be localized to cortical sites where actin and MTs interact in a Zw3-dependent manner (McCartney et al., 2001). However, exactly if and how these cortical proteins regulate the interaction between MTs, the nuclei, and the actin cortex remains unclear.

A major upstream regulator of GSK-3/Zw3 in higher eukaryotes is the oncogenic protein kinase Akt/PKB. Akt has well-established roles in cell growth, proliferation, and apoptosis and in mediating metabolic responses (Coffer et al., 1998). In addition, mammalian Akt has been shown to be phosphorylated at the G2/M transition and this phosphorylation corresponds to an increase in Akt activity throughout mitosis (Shtivelman et al., 2002; Wakefield et al., 2003). Signaling through phosphoinositide 3-kinase (PI3-K) by insulin or similar growth factors leads to translocation of Akt to the plasma membrane via a pleckstrin homology domain, where it is phosphorylated at two sites: a threonine residue in the catalytic domain and a serine residue at the C terminus of the protein (Andjelkovic et al., 1997). This results in activation of Akt, which transduces its cellular effects through substrate phosphorylation (Cross et al., 1995; Brunet et al., 1999; Dan et al., 2002). In the case of GSK-3/Zw-3, phosphorylation by Akt on a specific N-terminal residue leads to inactivation of GSK-3 activity (Shaw et al., 1997).

In this study, we provide evidence that Akt elicits its function in the early *D. melanogaster* embryo by phosphorylating and inactivating Zw3 and, through this, regulating the cortical complex of APC2–Arm. We show that embryos expressing reduced levels of Akt or those in which Akt has been inactivated by antibody injection fail to fully separate centrosomes before NEB. We also show that Akt is required for the localization of the MT + Tip protein EB1 to the embryonic cortex and that, in post-cellularized embryos, Akt is responsible for maintaining the orientation of mitotic spindles. Our results lead us to propose that, through regulating Zw3, Arm, APC2, and EB1, Akt normally maintains the stable interaction between MTs and the actin-rich cortex, facilitating both the final stages of dynein-dependent centrosome separation and correct spindle orientation.

Results

Akt is required for Zw3 phosphorylation during early *D. melanogaster* development

Unlike mammals, which possess three Akt genes, *D. melanogaster* has only one, *akt1*. A number of mutant alleles have been described: $akt1^{q}$ is an embryonic lethal null allele that leads to a nonfunctional protein possessing a point mutation in the ATP-binding domain of the kinase (Staveley et al., 1998), whereas $akt1^{04226}$ is a semilethal female sterility allele originally generated by the insertion of the P(PZ) transposon into the 5′ untranslated region of *akt*1 (Fig. 1 A; Spradling et al., 1999). We confirmed the *P* element insertion site using genomic DNA extracted from homozygous $akt1^{04226}$ adult flies (unpublished data) before analyzing the effect this *P* element had on the expression of Akt. We found these flies had dramatically reduced levels of *akt* mRNA (Fig. 1 B) and showed a concomitant reduction in Akt protein (Fig. 1 C). Although both egg chambers and oocytes possessed wild-type morphology (unpublished data), embryos laid by $akt1^{04226}$ homozygote mothers failed to hatch and arrested at varied stages of development. A proportion of these embryos could be clearly categorized as pre- or postcellularized (Table I). However, the majority consisted of two main classes: those that appeared to have a variable number of nuclei in the interior of the embryo and those that appeared to have cellularized but possessed wavy MT bundles and many hypercondensed nuclei (Fig. S1 A, available at http://www.jcb.org/cgi/content/full/jcb.200705085/DC1).

Akt transduces intracellular signals by phosphorylating target proteins, one of which is GSK-3. As the *D. melanogaster* GSK-3 homologue Zw3 (also known as *shaggy* or *sgg*) is highly expressed in embryos, we wondered whether Akt has a role in regulating Zw3 during the syncytial blastoderm. We generated antibodies specific for Zw3 phosphorylated on the conserved Akt site (Ser^{12} in *D. melanogaster*) and used them to assess the levels of phospho-Zw3 in embryos laid by wild-type and $akt1^{04226}$ flies. Affinity-purified antibodies recognized one clear band of ∼55 kD in wild-type embryo extracts that disappeared upon phosphatase treatment, which is consistent with phospho-Zw3 (Fig. S1 B and not depicted). However, in embryos laid by

Downloaded from www.jcb.org on February 15, 2008

Table I. **Developmental staging of akt^{04226} embryos**

	Precellularized	Postcellularized	Gastrulated	Other	*n*
	%	%	%	%	
Wild type	17	27	53	3	114
akt^{04226}	11	12	20	57	83

2–4-h-old wild-type and akt^{04226} embryos were fixed and stained for DNA and α-tubulin and the relative stage of development was assessed. Approximately half (53%) of wild-type embryos had undergone gastrulation, whereas the remaining embryos were either cellularized, undergoing gastrulation (27%), or had yet to cellularize (17%). The remaining 3% of embryos were empty of nuclei or MTs and appeared to be unfertilized. In contrast, only 21% of *akt* embryos appeared to have competed gastrulation.

$akt1^{04226}$ homozygote mothers, although total Zw3 levels remained unaffected, levels of phospho-Zw3 were dramatically reduced (Fig. 1 D).

The phosphorylation of Zw3 by Akt results in its inactivation. Thus, embryos laid by $akt1^{04226}$ homozygous mutants should possess more active Zw3. We therefore wondered whether reducing the activity of Zw3 in $akt1^{04226}$ mutants could rescue the maternal effect lethality. To test this, we used the sgg^{1} mutation, the result of an inversion within the Zw3 transcriptional unit and effectively a null allele in the early embryo (Ruel et al., 1993), to genetically alter the levels of Zw3 in an *akt* mutant background. We found that although all $akt1^{04226}$-derived embryos failed to hatch, 79% of *akt* embryos laid by mothers carrying a copy of the sgg^{1} mutation (sgg^{1}/FM7; $akt1^{04226}$ flies) were viable (Fig. 1 E). This is comparable to the 77% hatch rate of embryos laid by sgg^{1}/FM7 flies (Fig. 1 E). Together, these results show that Akt is essential for Zw3 phosphorylation and suggest that the only essential maternal role of Akt in early *D. melanogaster* development is the phosphorylation of Zw3.

akt mutant embryos display nuclear fallout and bent mitotic spindles

To investigate the role of Akt during syncytial development, we fixed and stained 1–3-h-old embryos laid by *akt* mutant mothers to visualize DNA, MTs, and centrosomes. To ensure that the nature of the maternal effect lethality reflects a requirement for Akt protein, we generated heteroallelic flies with the genotype $akt1^{q}/akt1^{04226}$. $akt1^{q}/akt1^{04226}$ flies display maternal effect lethality comparable to $akt1^{04226}/akt1^{04226}$ individuals, and all analyses described in this study unless otherwise stated were performed on $akt1^{q}/akt1^{04226}$ embryos (henceforth termed *akt* embryos). Two main differences to wild-type embryos could be discerned. First, although nuclei were arranged with regular spacing in wild-type embryos, *akt* embryos showed patches of the cortex devoid of nuclei (Fig. 2, A and B). These patches often still contained centrosomes, which implies that nuclear migration had been successful but that nuclei had subsequently moved into the interior of the embryo (Fig. 2 B). Second, spindles in *akt* embryos

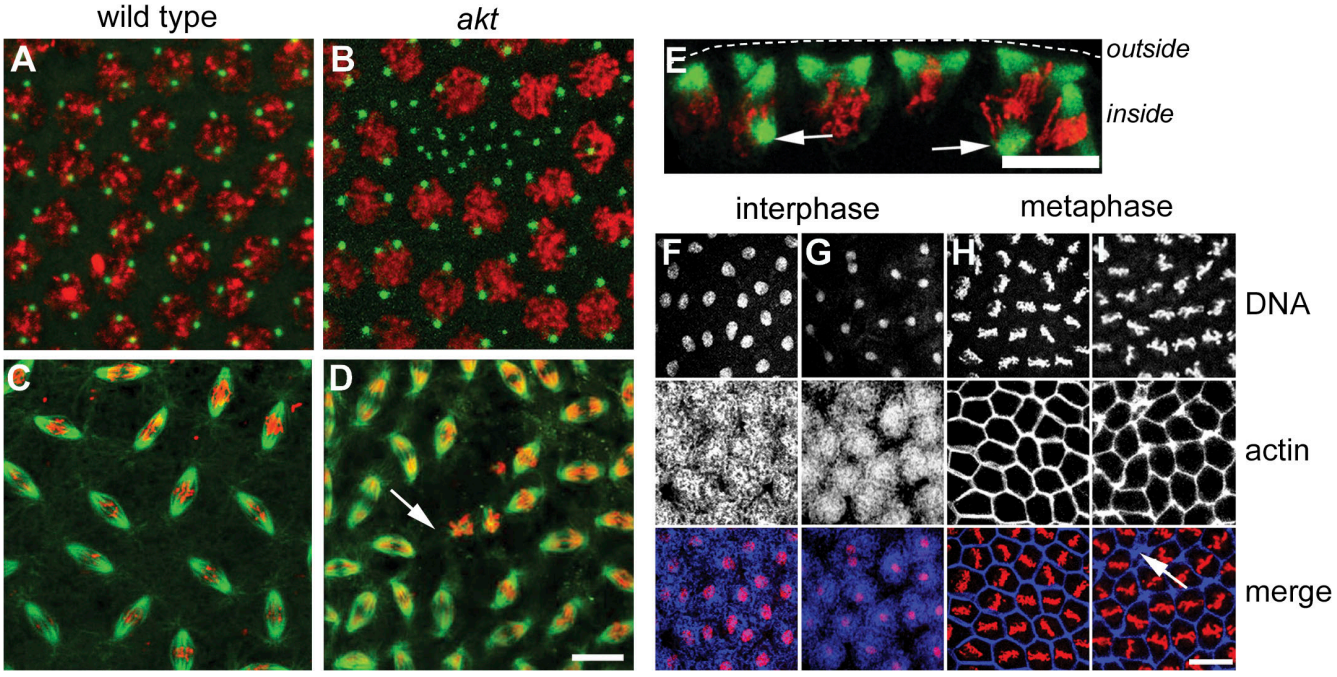

Figure 2. **Reduced Akt levels lead to defects in syncytial mitoses.** (A–D) Syncytial stage embryos fixed with methanol to reveal DNA (red), centrosomes (A and B, green), or MTs (C and D, green). (A and C) Wild-type embryos. (B and D) *akt* embryos show gaps in their cortex, which is devoid of nuclei but contains many centrosomes. Although many spindles look normal, regions of *akt* embryos show poorly formed spindles that are irregularly spaced (D, arrow). (E) A cross-sectional view of an *akt* embryo in prometaphase. Arrows indicate spindle poles not connected to the embryonic cortex. (F–I) Gross actin morphology is not perturbed in *akt* embryos. During interphase in wild-type (F) or *akt* embryos (G), actin is present in cortical caps. During metaphase in wild-type (H) and *akt* (I) embryos, actin is present in pseudocleavage furrows. Bars, 10 μm.

Downloaded from www.jcb.org on February 15, 2008

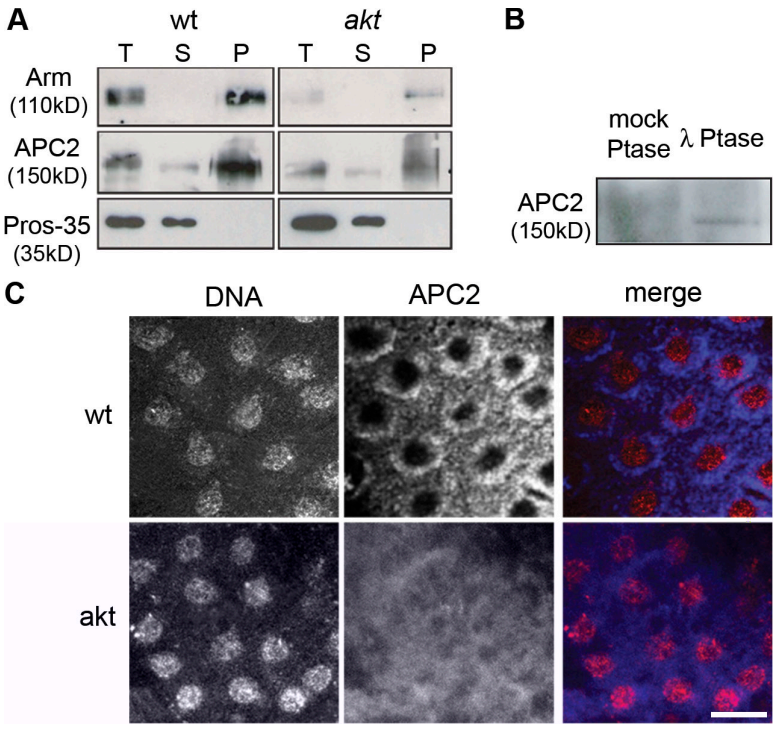

Figure 3. **The regulation of APC2 and Arm is altered in *akt* embryos.** (A) Immunoprecipiation of Arm from 0–3-h wild-type and *akt*1^{04226} embryo extracts. Pros-35 is shown as a control. T, total extract; S, supernatant; P, pellet. (B) The mobility of APC2 in *akt*1^{04226} embryos can be altered by treatment with λ phosphatase. (C) Wild-type and *akt*1^{04226} embryos fixed and stained to visualize DNA and APC2. In *akt* embryos, APC2 fails to localize. Bar, 10 μm.

were occasionally bent or short (Fig. 2, C–E). Cross-sectional views of these embryos also showed spindles that appeared to be attached to the cortex by only one pole (Fig. 2 E, arrows).

Several maternal effect mutations have been identified that display such a nuclear fallout defect after cortical migration (Sullivan et al., 1993). This phenotype can be reproduced by treatment with cytochalasin B, which inhibits actin polymerization, and is consistent with defects in cortical F-actin recruitment or organization (Rothwell et al., 1998). However, we found that *akt* embryos had the ability to localize actin to both caps during interphase and the pseudocleavage furrows during mitosis (Fig. 2, F–I). Additionally, in areas of the embryo where nuclei had fallen in, actin still localized to pseudocleavage furrows organized by persisting centrosomes (Fig. 2 I, arrow). Taken together, these results suggest Akt normally has a role in regulating the interaction between nuclei and the cortex during the syncytial divisions without affecting gross actin morphology.

Akt regulates the stability and localization of a cortical complex containing E-APC and Arm

Previously published work has shown that during syncytial mitoses, Zw3 acts to regulate the localization of a complex containing Arm (the *D. melanogaster* homologue of β-catenin) and the APC-related protein APC2/E-APC (McCartney et al., 2001; Cliffe et al., 2004). In addition, embryos laid by females homozygous for a mutation in the *apc2* gene resulting in the deletion of the Arm-binding repeats (*apc2*$^{\Delta 5}$) also displayed patches of embryonic cortex devoid of nuclei (McCartney et al., 2001). Therefore, we decided to investigate whether Akt has a role in regulating the Arm–APC2 complex through Zw3 during embryogenesis. By immunoprecipitating Arm from wild-type and *akt*1^{04226} embryo extracts, we were able to coprecipitate APC2 (Fig. 3 A). However, although Arm and APC2 were complexed both in wild-type and *akt*1^{04226} extracts, total levels of Arm were substantially reduced in *akt*1^{04226} extracts (Fig. 3 A). Additionally, Arm-associated APC2, which ran as a single band on Western blots in wild-type embryos, was present as a smear in *akt*1^{04226} embryos (Fig. 3, A and B). This extended mobility could be reversed upon incubation with λ phosphatase, possibly suggesting that APC2 is highly phosphorylated in embryos deficient in Akt (Fig. 3 B). To further address what effect decreased Akt activity might have on this complex, we compared the localization of APC2 in wild-type and *akt* embryos. During interphase in wild-type embryos, APC2 was present at the embryonic cortex, as has been found previously (Fig. 3 C; McCartney et al., 1999; Townsley and Bienz, 2000; McCartney et al., 2001). However, in *akt* embryos, this cortical localization was disrupted and APC2 was found entirely in the cytoplasm (Fig. 3 C). Thus, in the early embryo, Akt appears to regulate the proteins levels of Arm and the localization of APC2.

Akt localizes to the embryonic cortex in a cell cycle–dependent manner

Activated Akt is known to associate to the plasma membrane using its conserved pleckstrin homology domain. As commercial antibodies that recognize *D. melanogaster* Akt in Western blots failed to show any specific localization in early embryos (unpublished data), we investigated the localization of Akt in flies expressing an Akt-turbo-GFP fusion protein using the maternal UAS/Gal4 system (see Materials and methods). 0–3-h embryos collected from nanos-Gal4:UAS-Akt-tGFP flies (hereafter termed Akt-tGFP embryos) express Akt-tGFP at levels similar to that of endogenously expressed Akt (Fig. 4 A). Live analysis of cycle 12 Akt-tGFP embryos showed that Akt-tGFP localized to cortical patches, which is reminiscent of actin caps

Downloaded from www.jcb.org on February 15, 2008

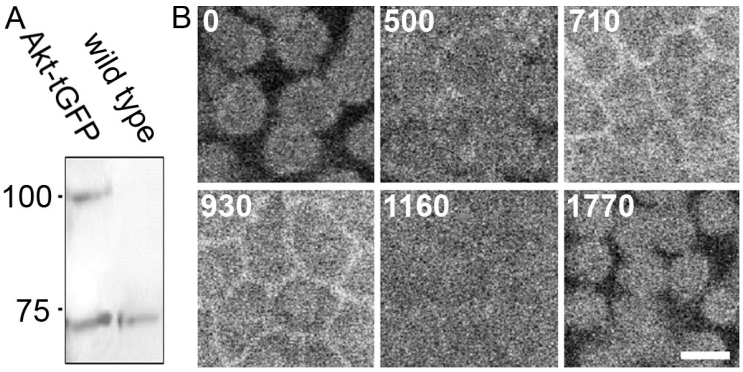

Figure 4. **Akt localizes to the embryonic cortex in a cell cycle–dependent manner.** (A) Western blot of 0–3-h wild-type embryos and embryos containing UAS-Akt-turbo-GFP driven by Nanos Gal4. Akt-tGFP is expressed at similar levels to endogenous Akt. Molecular mass (kD) is indicated on the left. (B) Live confocal analysis of embryos expressing Akt-tGFP under the UAS-Gal4 system. Akt-tGFP appears to cycle between cortical caps (0 and 1,770 s) and pseudocleavage furrows (710 and 930 s). Time is indicated in seconds. See Video 1 (available at http://www.jcb.org/cgi/content/full/jcb.200705085/DC1). Bar, 10 μm.

during interphase (Figs. 2 F and 4 B; and Video 1, available at http://www.jcb.org/cgi/content/full/jcb.200705085/DC1; Sullivan and Theurkauf, 1995). As the cycle progressed, these caps spread and migrated away from the cortex until they become enriched in hexagonal arrangements that appeared similar to metaphase pseudocleavage furrows. Eventually these hexagons extended before dissolving completely. Akt-tGFP localization then returned to cortical caps (Fig. 4 B and Video 1). Thus, Akt is dynamically recruited to the embryonic cortex with similar dynamics to actin, placing it in the correct subcellular location to regulate Zw3, Arm, and APC2.

akt and *apc2*^{1S} embryos show defects in centrosome separation

To investigate the defects in mitosis observed in fixed *akt* embryos in more detail, we analyzed nuclei, MT, and centrosome dynamics using time-lapse confocal microscopy. In wild-type embryos expressing histone H2B-GFP, the synchronous mitoses occur with high fidelity, although nuclei occasionally (0.8%, $n = 1{,}357$) move into the interior of the embryo (Fig. 5 A and Video 2 available at http://www.jcb.org/cgi/content/full/jcb.200705085/DC1). In agreement with our observations in fixed cells, *akt* embryos showed an approximately fivefold increase in nuclear fallout (3.7%, $n = 1.953$; Fig. 5 A and Video 3). However, a quantitative analysis of chromosome dynamics showed that key mitotic parameters such as the rate of chromosome condensation, the length of time spent in metaphase, and the rate of chromosome segregation were similar in both wild-type and *akt* embryos (Fig. 5, B and C).

In wild-type embryos expressing α-tubulin–GFP, nuclei can also be followed as dark circles in which soluble tubulin is excluded. (Fig. 6 A and Video 4, available at http://www.jcb.org/cgi/content/full/jcb.200705085/DC1). During telophase and interphase, centrosomes migrate around nuclei until they lie approximately opposite one another (Robinson et al., 1999). After NEB, MTs invade the nucleus, capture chromosomes, and form a stable bipolar mitotic spindle (Video 4). To compare the MT dynamics in wild-type and *akt* embryos, we developed software able to identify and track the nuclei in which tubulin is excluded and the foci of fluorescent tubulin corresponding to the centrosomes. This package is based on similar principles to those previously described for our automated chromosome tracking software and allows specific biologically relevant parameters to be determined without observer error or bias (see Materials and methods; Yau and Wakefield, 2007).

We found no gross morphological differences in MT organization between wild-type and *akt* embryos. However, whereas in wild-type embryos the mean centrosome separation angle just before NEB was 170° (SEM ± 0.79°, $n = 100$), the mean angle in *akt* embryos was 157° and varied greatly between individual nuclei; we obtained angles of between 106 and 180° (SEM ± 1.77°, $n = 100$; Fig. 6, A and B; Table II; and Video 5, available at http://www.jcb.org/cgi/content/full/jcb.200705085/DC1). Additionally, the percentage of nuclei possessing centrosomal pairs with angles <150° just before NEB was clearly different between wild-type and *akt* embryos; although only 2% of wild-type centrosomal pairs had separated to <150° by NEB, this number increased to 30% in *akt* embryos (Table II).

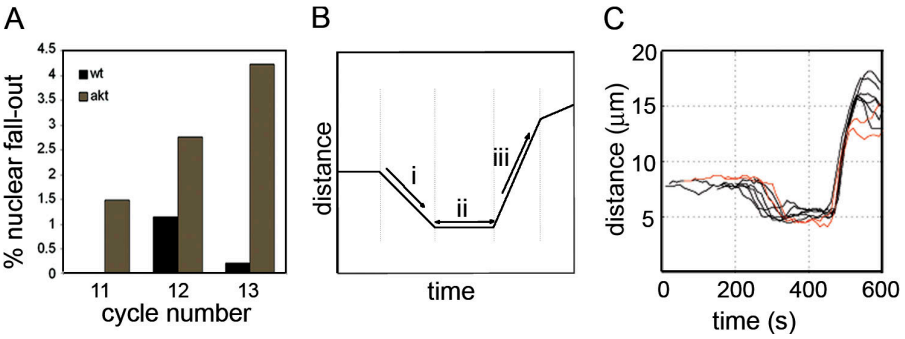

Figure 5. **The timing of syncytial mitoses is not affected in *akt* embryos.** Chromosome dynamics in wild-type and $akt1^{q}/akt1^{04226}$ embryos expressing GFP-histone. (A) Histogram representing the percentage of nuclei that move into the interior of the embryo (nuclear fallout) during cycles 11, 12, and 13. Data were obtained from 20 wild-type and 20 $akt1^{q}/akt1^{04226}$ embryos. (B) Graphical representation of an idealized graph applied to chromosomes throughout mitosis (Yau and Wakefield, 2007). Parameters of interest are automatically obtained using this software, such as (i) rate of chromosome condensation, (ii) length of metaphase, and (iii) rate of chromosome segregation. (C) Chromosome dynamics during cycle 12 in wild-type (black) and $akt1^{q}/akt1^{04226}$ (red) embryos. Each line is the mean of 10 nuclei from a single embryo. Data were obtained from seven different wild-type or $akt1^{q}/akt1^{04226}$ embryos. Similar results were found for embryos in cycles 11 and 13 (unpublished data). See Videos 2 and 3 (available at http://www.jcb.org/cgi/content/full/jcb.200705085/DC1).

Downloaded from www.jcb.org on February 15, 2008

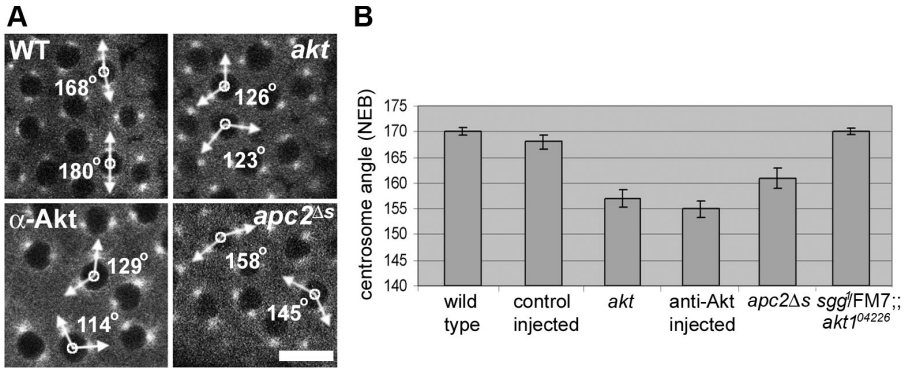

Figure 6. **Centrosome separation is inhibited after inactivation of Akt or APC2.** (A) Live confocal analysis of embryos expressing α-tubulin–GFP. Examples of the angle of centrosome separation 20 s before NEB in wild-type (WT) embryos, *akt1*^{q}/*akt1*^{04226} embryos (*akt*), embryos injected with anti-Akt antibodies (α-Akt), and embryos expressing an allele of APC2 unable to bind to Arm (*apc2Δs*). Bar, 10 μm. (B) Histogram representing the mean angle of centrosome separation before NEB in embryos. Data for each class was obtained from 100 individual nuclei. Errors bars indicate the SEM. See Videos 4–8 (available at http://www.jcb.org/cgi/content/full/jcb.200705085/DC1).

We confirmed the effect of reduced levels of Akt on centrosome separation using antibody injection experiments. Anti-Akt antibodies were injected into 1–2-h-old wild-type embryos expressing α-tubulin–GFP and immediately imaged (Fig. 6, A and B; and Video 6, available at http://www.jcb.org/cgi/content/full/jcb.200705085/DC1). To monitor for any defects observed associated with injection, we also analyzed MT organization in control-injected embryos (Video 7). In good agreement with our mutational analysis, the mean angle of centrosome separation just before NEB was 153° in anti-Akt antibody–injected embryos (SEM ± 1.63, $n = 100$), whereas 27% of nuclei possessed centrosomes that had separated <150° at NEB (Fig. 6, A and B; and Table II).

Given the evidence for a role for Akt in regulating the localization of APC2 (Fig. 3) and the similarity in fixed phenotypes between *akt* and *apc2*$^{\Delta S}$ mutants (Fig. 2; McCartney et al., 2001), we next analyzed centrosome separation in live *apc2*$^{\Delta S}$ embryos. Again, we found a significant effect when compared with wild-type embryos; the mean angle of centrosome separation in homozygote *apc2*$^{\Delta S}$ embryos was 159° (SEM ± 2.02, $n = 100$) with 16% of nuclei possessing centrosomes that had separated <150°, which was eightfold more than expected for wild-type embryos (Fig. 6, A and B; Table II; and Video 8, available at http://www.jcb.org/cgi/content/full/jcb.200705085/DC1).

Finally, to confirm that Akt acts through Zw3 in the syncytial blastoderm, we analyzed the angle of centrosome separation in *akt* embryos laid by mothers possessing only one copy of wild-type Zw3 (*sgg*^{1}/FM7; α-tubulin–GFP; *akt1*^{04226} flies). These embryos showed no significant cortical patches lacking nuclei and the mean angle of centrosome separation just before NEB was 168° (SEM ± 0.76°, $n = 50$; Fig. 6, A and B; Table II; and not depicted). Thus, reducing the amount of Zw3 in an *akt* mutant background rescues the centrosome separation defect.

Together, these results show that reducing the activity of Akt in the syncytial blastoderm results in impaired centrosome migration around cortical nuclei, a specific effect that is transduced through Zw3 and is also consistently observed in embryos in which the interaction between APC2 and Arm has been disrupted (i.e., *apc2*$^{\Delta S}$ embryos).

The dynamics of centrosome separation are altered in *akt* embryos

To analyze the exact cause of the impaired centrosome migration seen in *akt* embryos, we used our software to track the centrosomes over time. In agreement with previously published data, separation of centrosomes during interphase in wild-type cycle 12 embryos appeared to be composed of two components (Fig. 7 A; Sharp et al., 2000; Cytrynbaum et al., 2003). An initial fast hyperbolic separation led to an intercentrosomal distance of 4–5 μm. This was followed by a near linear rate of 0.01 μm/s, resulting in full separation of centrosomes by 6–7 μm just before NEB (Fig. 7 A and Video 4). We found that the profile of centrosome separation in *akt* embryos differed from the wild type in two respects. First, the mean initial rate of separation appeared to be slower. Second, the secondary, linear rate of separation appeared to be absent. Consequently, centrosomes completed their movements ∼240 s before NEB, after they had reached a separation of ∼4–5 μm, and remained at this approximate distance

Table II. **Inactivation of Akt or APC2 leads to defects in centrosome migration**

	Wild type	Control injected	*akt* mutant	α-Akt injected	*Apc2*$^{\Delta S}$ mutant	*sgg*^{1}/FM7;; *akt* mutant
Mean angle of centrosome separation	170	168	155	157	161	168
SEM centrosome separation	0.79	1.04	1.77	1.63	2.02	0.73
Percentage of nuclei with centrosome angle <150°	2	8	27	30	16	2

Cycle 12 embryos expressing α-tubulin–GFP were imaged every 10 s under the confocal microscope. Image series were analyzed using automated tracking software and the angle of centrosome separation 20 s before NEB was calculated. *akt* mutant, embryos laid by *akt*^{04226}/*akt1*^{q} mothers; α-Akt injected, embryos injected with Alexa 555–labeled anti-Akt antibodies; *apc2*$^{\Delta s}$ mutant, embryos laid by *apc2*$^{\Delta s}$ homozygote mothers; control injected, embryos injected with Alexa 555–labeled BSA; *sgg*^{1}/FM7;; *akt* mutant, embryos laid by *akt*^{04226}/*akt1*^{q} mothers carrying one copy of the *sgg*^{1} mutation; wild type, wild-type embryos.

Downloaded from www.jcb.org on February 15, 2008

away from each other until after NEB (Fig. 7 A and Video 5). Of these two differences, however, only the second was statistically significant. Thus, although centrosome separation may be compromised in *akt* embryos in general, it is the terminal stages of this process that are clearly altered in comparison to wild-type embryos.

During cycles 10 and 11 in *akt* embryos, just as centrosomes and nuclei complete their migration to the embryonic cortex, we also observed some nuclei that possessed a centrosome that detached from the nuclear envelope and moved away from the nucleus and sister centrosome. Upon NEB, the remaining attached centrosome formed a monocentrosomal bipolar spindle that subsequently recaptured the wandering centrosome during metaphase (Fig. 7 C and Video 9, available at http://www.jcb.org/cgi/content/full/jcb.200705085/DC1). Again, this phenotype was consistently observed not only in *akt* embryos but also in those in which Akt had been inactivated through antibody injection (Fig. 7 C and Video 10). A direct consequence of this abnormal centrosome migration was the formation of short or bent spindles (Fig. 7, C and D; and Videos 9 and 10). Although in all observed cases, spindle morphology was rescued before anaphase, the resultant nuclei sometimes moved from the cortex to the interior of the embryo during the following interphase.

Together, these results are consistent with the analysis of fixed embryos, in which bent and short spindles and spindles attached to the cortex by one pole were observed (Fig. 2, D and E). They show that Akt normally has a role in ensuring the completion of centrosome separation in the syncytial blastoderm embryo and suggest that the nuclear fallout seen in *akt* embryos could result, at least partly, from defects in centrosome migration.

Akt is required for the cortical localization of the MT + Tip protein EB1

It has previously been suggested that the cortical APC2–Arm complex might interact with MTs through the conserved MT + Tip protein EB1 (Allan and Nathke, 2001). *D. melanogaster* EB1 has multiple roles in centrosome migration, spindle formation, and kinetochore function (Rogers et al., 2002). Mammalian EB1 and APC have been shown to directly bind one another and act together during chromosome alignment (Su et al., 1995; Green et al., 2005). EB1 has also been shown to be capable of interacting with the MT motor protein dynein, which, during syncytial development, is present at the cortex and provides the force required for centrosome separation (Berrueta et al., 1999; Sharp et al., 2000; Cytrynbaum et al., 2003). To investigate whether Akt acts on centrosome separation through EB1, we fixed wild-type and *akt* embryos with formaldehyde and stained them with antibodies specific to *D. melanogaster* EB1. In wild-type embryos, EB1 localized to spindles during metaphase, showing enrichment at the plus ends of MTs as described previously (Fig. 8 A; Rogers et al., 2002). During interphase, however, EB1 was present both at centrosomes and the embryonic cortex, where it was enriched at the actin caps (Fig. 8 B). As a second specific antibody to EB1 gave identical results, this cortical localization is unlikely to be a fixation artifact (unpublished data). In *akt* embryos, although the localization of EB1 to MTs and centrosomes during metaphase and interphase was unperturbed, the cortical enrichment at the actin caps during interphase was completely abolished (Fig. 8, C and D). Akt therefore appears to be required for the cortical localization of EB1.

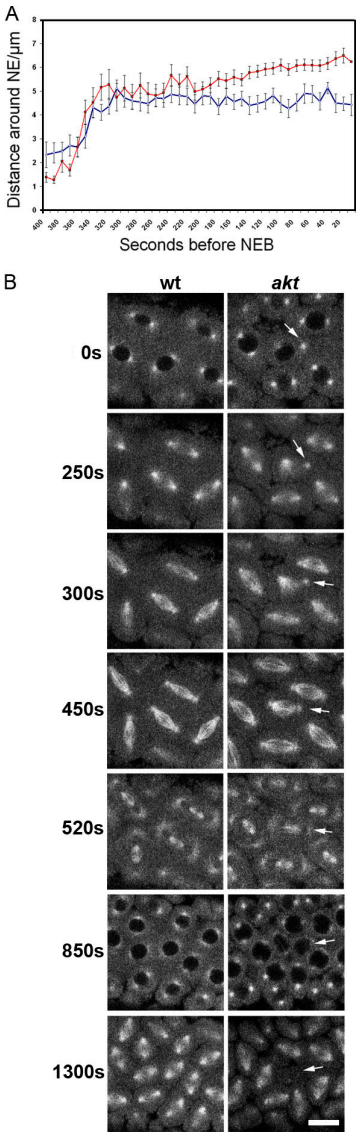

Figure 7. **The dynamics of centrosome migration in *akt* embryos.** (A) Purpose designed automated tracking software was used to identify and follow centrosome movement in wild-type or *akt* embryos. Data were obtained from 26 wild-type and 16 $akt1^{q}/akt1^{04226}$ centrosomal pairs. Error bars show the SEM based on one standard deviation. (B) Stills from time-lapse videos of cycle 11 wild-type (wt) and $akt1^{q}/akt1^{04226}$ (*akt*) embryos. In the *akt* embryo, a centrosome that appears to have detached from the nuclear envelope does not initially contribute to spindle formation (arrows). The bent, short spindle formed recaptures the centrosome and is capable of chromosome segregation. Nonetheless, the resulting nuclei move into the interior of the embryo during the following interphase. See Videos 9 and 10 (available at http://www.jcb.org/cgi/content/full/jcb.200705085/DC1). Bar, 10 µm.

Akt regulates spindle orientation and APC2 localization in postcellularized embryos

As some *akt* embryos complete cellularization and undergo normal gastrulation (Table I), we also investigated whether mitotic

Downloaded from www.jcb.org on February 15, 2008

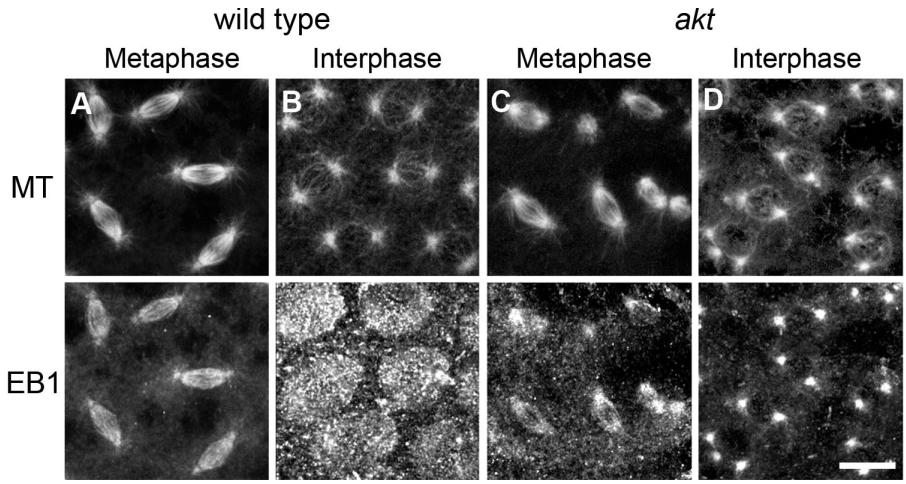

Figure 8. **The localization of EB1 is altered in *akt* embryos.** Wild-type (A and B) and $akt1^{04226}/akt1^{04226}$ (C and D) embryos fixed and stained with antibodies to α-tubulin and EB1. The ability of EB1 to bind centrosomes and spindles during metaphase is similar in wild-type and *akt* embryos. However, although wild-type embryos accumulate EB1 at the embryonic cortex and at centrosomes during interphase, *akt* embryos only accumulate EB1 on centrosomes. Bar, 10 μm.

cells in embryos exhibit any defects in spindle formation. 2–4-h-old wild-type and *akt* embryos were fixed and stained for α-tubulin to show MTs (Fig. 9, A and B). After cellularization, mitosis occurs asynchronously in specific mitotic domains (Foe, 1989). Importantly, in wild-type embryos, these cell divisions are usually oriented parallel to the surface of the embryo (Fig. 9 A). However, when we investigated the morphology of spindles from *akt* embryos, we found they were not uniformly oriented in relation to the cortex (Fig. 9 B). Images taken along the z axis of embryos at 1-μm intervals were used to assess the relative vertical displacement of the two poles. In wild-type embryos, the mean vertical displacement between the two spindle poles was ∼1 μm (Fig. 9 C). By assuming a mean spindle length of 10 μm pole-to-pole, this corresponds to a typical orientation of 6° from the horizontal (Fig. 9 D). In *akt* embryos, the mean vertical displacement between spindle poles was ∼5 μm (Fig. 9 C). This displacement varied widely, with some spindles having both poles in the same plane and some apparently perpendicular to the plane of the epithelium. The mean vertical displacement in *akt* embryos corresponds to a spindle at an angle of 29° to the horizontal (Fig. 9 D).

Finally, as APC2 has been shown to be necessary for MT–cortex interactions and spindle orientation in a variety of *D. melanogaster* cell types (Lu et al., 2001; McCartney et al., 2001; Yamashita et al., 2003), we assessed whether Akt regulates APC2 in cellularized tissues in addition to the syncytial blastoderm. We fixed 2–4-h-old embryos in formaldehyde and stained for APC2 and MTs. In wild-type mitotic domains, APC2 was enriched at the cell periphery, which is consistent with previously published data (Fig. 9 E; Yu et al., 1999). In postcellularized *akt* embryos, similarly to syncytial embryos, cortical APC2 localization was significantly weakened or totally abolished (Fig. 9 F). Together, these results show that Akt normally has a role in postcellularized *D. melanogaster* embryos regulating spindle orientation and cortical APC2.

Discussion

Using a combination of live and fixed imaging of *D. melanogaster* embryos, the work described in this study reveals a novel role for Akt in regulating centrosome migration. Genetic, biochemical, and immunolocalization studies suggest that Akt exerts its effects by phosphorylating and inhibiting Zw3 and, through this process, regulating a cortical complex of APC2–Arm and the MT + Tip protein EB1. The dynamic localization of an Akt-tGFP fusion protein to actin-rich cortical structures is consistent with a role in maintaining actin-associated APC2–Arm complexes. Furthermore, we have provided evidence for a role for Akt in maintaining spindle orientation in cellularized embryonic epithelia, possibly through regulating the association between APC2 and the embryonic cortex.

A specific role for Akt in regulating centrosome separation through Zw3, APC2, Arm, and EB1

We began this study by investigating the phenotype of embryos laid by mothers that are transheterozygous for two different alleles of the *D. melanogaster akt1* gene, the maternal effect $akt1^{04426}$ allele and the early embryonic lethal null $akt1^{q}$. Both fixed and live analyses show that these mutant embryos exhibit specific defects in centrosome separation, spindle morphology, and a nuclear fallout phenotype that is actin independent. All the evidence we provide can be explained by effects transduced through one specific signal transduction pathway in which Akt phosphorylates and inactivates Zw3, which, in turn regulates cortical APC2, Arm, and EB1. However, given the many potential substrates of Akt in the early embryo, is it possible to reach this conclusion?

Akt has a clearly defined metabolic role in storage of macromolecules (Cong et al., 1997; Cross et al., 1997). It is therefore conceivable that the energy stores laid down in *akt* embryos by mutant mothers are insufficient for the syncytial blastoderm to complete all mitoses without affecting MT and centrosome dynamics. However, mutations in other genes regulating metabolism affect many different aspects of mitosis, including the synchrony of divisions, making this possibility unlikely (Frenz and Glover, 1996). Akt also functions in regulating translation (Coffer et al., 1998). Although it is possible that the phenotype observed in *akt* mutants is caused by an inability to translate specific proteins, all other proteins analyzed in this study (e.g., CP190, tubulin, and Pros-35) are present at similar levels in both wild-type and *akt* embryos. Furthermore, Akt has a role in

Downloaded from www.jcb.org on February 15, 2008

the regulation of cell cycle progression and constitutively active Akt can phosphorylate the checkpoint protein Chk1 in vitro (Shtivelman et al., 2002). However, our quantitative analysis of chromosome dynamics shows that key mitotic parameters are unaffected in *akt* embryos (Fig. 5). Perhaps conclusively, the effect on centrosome separation observed in *akt* mutants is phenocopied in embryos in which Akt is inhibited by antibody injection directly before imaging. This strongly suggests that indirect, cumulative effects of reduced Akt activity over the first few hours of *D. melanogaster* development cannot account for the defects observed in centrosome migration.

Previously published work has shown that APC2 and Arm have a role in maintaining interactions between the cortex and mitotic spindles and that Zw3 regulates Arm and APC2 localization in the early embryo (McCartney et al., 2001; Cliffe et al., 2004). In this study, we have shown that: (i) Akt is essential for Zw3 phosphorylation, (ii) Akt localizes to the cell cortex, (iii) Akt is responsible for the cortical localizations of APC2 and EB1 and the levels of embryonic Arm protein, (iv) *akt* mutant embryos and embryos in which Akt has been specifically disrupted using antibody injections show a reproducible defect in centrosome separation, leading to bent and short spindles, (v) this phenotype can be rescued by reducing the levels of Zw3, and (vi) $apc2^{\Delta S}$ embryos show an identical centrosome separation phenotype. Thus, although we cannot formally rule out other roles for Akt in the early embryo, the evidence points to a specific role for Akt in regulating the interaction between centrosomes and the embryonic cortex during the syncytial mitoses through regulating Zw3, Arm, APC2, and EB1.

The role of Akt in regulating wingless signaling components

In the early embryo, Akt is responsible for phosphorylating Zw3 on a conserved N-terminal residue (Ser^{12} in *D. melanogaster* Zw3, Ser^{9} in human GSK3α, and Ser^{21} in human GSK3β). GSK3/Zw3 is normally active within resting cells and phosphorylation on this site by Akt upon activation of the PI3-K signaling pathway is well-documented to inactivate the kinase (Cross et al., 1995). Zw3 is also inactivated by phosphorylation on a different inhibitory site upon activation of the Wingless signaling pathway (Peifer and Polakis, 2000). Active (unphosphorylated) Zw3 normally phosphorylates both APC and Arm, resulting in efficient targeting of Arm for proteolysis. Inhibition of Zw3 in this context leads to a stabilization and concomitant accumulation of Arm, allowing it to translocate into the nucleus, where it regulates transcription of Wingless-specific genes (Peifer and Polakis, 2000).

Although the PI3-K and Wingless signaling pathways do not converge on Zw3 and it is not generally thought that phosphorylation of Zw3 on Ser^{12} affects Wingless signaling (Papadopoulou et al., 2004), phosphorylation on this site has previously been shown to regulate GSK-3–dependent phosphorylation of APC (Etienne-Manneville and Hall, 2003; Zhou et al., 2004). Given that *akt* mutant embryos, which possess unphosphorylated (active) Zw3, contain both more highly phosphorylated APC2 and dramatically lower levels of Arm protein compared with wild-type embryos, our data seems to provide an example in *D. melanogaster*, whereby regulation of Zw3 may facilitate cross-talk between PI3-K and Wingless signaling targets.

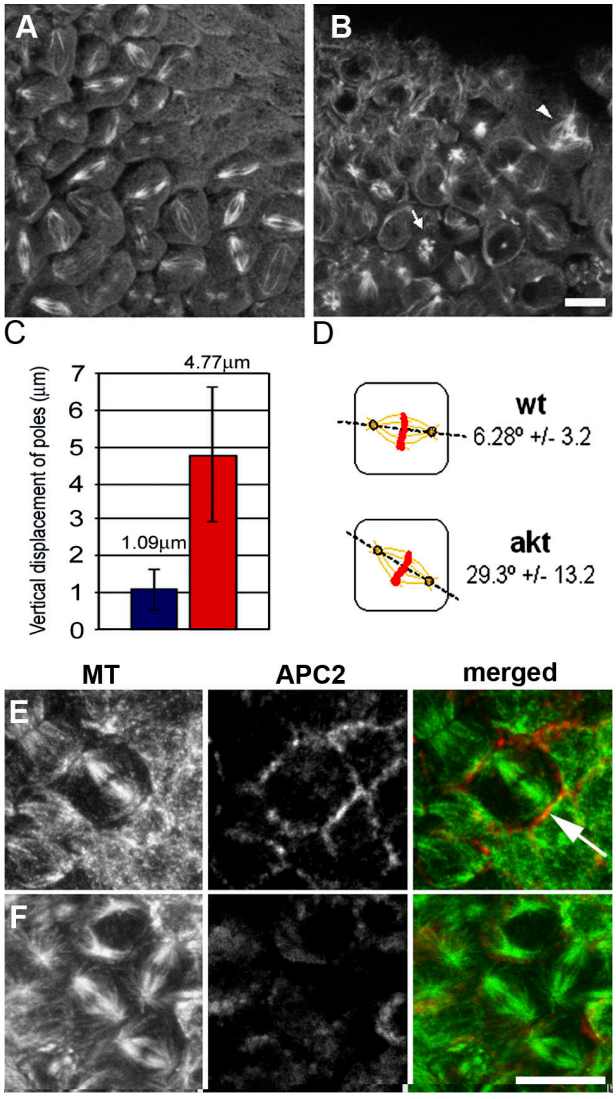

Figure 9. **The axis of spindle formation is perturbed in cellularized akt embryos.** (A and B) Single plane confocal analysis of 2–4-h wild-type and $akt1^{04226}$ embryos fixed and stained with anti-tubulin antibodies. (A) Mitotic spindles in wild-type embryos appear parallel to the embryonic cortex. (B) In akt embryos, mitotic spindles are positioned in many different orientations. (C) Quantitative analysis of spindle orientation in wild-type and *akt* embryos. Data were obtained from 100 spindles from four wild-type and *akt* embryos. Error bars indicate the SEM. Blue, wild-type embryos; red, akt embryos. (D) Diagram of the results shown in C. (E and F) 2–4-h wild-type (E) and $akt1^{04226}$ (F) embryos fixed and stained with antibodies to α-tubulin and APC2. Arrows indicate mitotic spindles oriented perpendicular to the most embryonic cortex. Bar, 10 μm.

The molecular role of Akt in centrosome separation

Embryos containing reduced levels of active Akt show a specific, reproducible affect on centrosome separation, significantly perturbing the final, slow phase of migration around the nuclear envelope. Although the effect is subtle (embryos in which either dynein or the MT motor Klp61F function has been inactivated completely fail to separate centrosomes; Sharp et al., 2000), ~30% of centrosomal pairs in *akt* embryos are separated by <150° by NEB. In contrast, 98% of centrosomal pairs in wild-type embryos achieve this degree of separation. What, then, might be the cause underlying this partial inhibition?

Downloaded from www.jcb.org on February 15, 2008

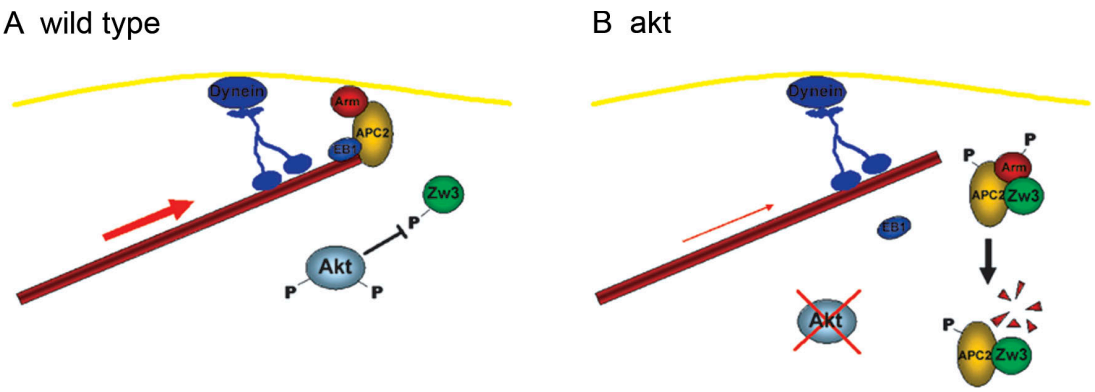

Figure 10. **A model of how Akt contributes to centrosome separation in the syncytial blastoderm.** (A) In wild-type embryos, cortical Akt phosphorylates Zw3, ensuring it remains inactive. A complex of Arm and APC2 is able to interact with the actin cortex and with the MT + Tip protein EB1. The stable interaction between the cortex and MTs allows cortical dynein to generate the force required for full centrosome separation. (B) In embryos in which *akt* levels are severely reduced, Zw3 is no longer phosphorylated. The active Zw3 kinase can now phosphorylate both APC2 and Arm. Phosphorylated Arm is targeted for degradation, disrupting the cortical complex. EB1, although able to bind MTs, cannot stably associate with the actin cortex in the absence of cortical Arm–APC2. Cortical dynein is able to transiently interact with MTs and generate force. However, the force required for full centrosome separation is now greater than can be generated in the absence of Arm–APC2. Consequently, centrosome separation stops before completion.

Cortical dynein is known to be required during all stages of centrosome separation, generating a force between the cortex and the MTs linking the cortex that increases as centrosomes progressively separate (Sharp et al., 2000; Cytrynbaum et al., 2003, 2005). Moreover, experimental investigation and mathematical modeling of force generation during *D. melanogaster* embryonic mitoses provides compelling evidence that the centrosomal pairs complete their separation because of outward forces on the spindle originating at the cortex (Cytrynbaum et al., 2005). One explanation of the *akt* phenotype is that cortical Akt normally contributes to the final stages of centrosome separation by regulating the interaction between the embryonic cortex and the mitotic spindle through directly phosphorylating Zw3 and, through this, regulating Arm, APC2, and EB1.

In our model, we suggest that during the initial stages of centrosome separation, cortical dynein is able to act on MTs that transiently associate with the cell cortex (Fig. 10, A and B). However, as centrosomes continue to separate, the MTs require a more stable interaction with the cortex to contend with the increased force acting upon them. Through phosphorylating and inactivating Zw3 at the embryonic cortex, Akt would maintain sufficient levels of Arm and APC2 at the cortex facilitating a stable interaction with EB1 and MTs. Dynein can therefore continue to exert force on the cortex, centrosomes, and nuclear envelope, and centrosome separation can progress to completion (Fig. 10 A). In *akt* mutants, Zw3 is derepressed, allowing it to phosphorylate and disrupt the cortical complex. Arm is degraded, cortical APC2 and EB1 are lost, and MTs are only transiently associated with dynein. Consequently, the force generated during the final stages of centrosome separation would be insufficient for full separation and centrosomes would stall (Fig. 10 B).

A general role for Akt in regulating MT–cortical interactions

In polarized tissues such as the *D. melanogaster* neuroectoderm, adherens junctions provide the dominant cue for spindle orientation, allowing the epithelial cells to divide along their apical–basal axis. Interestingly, APC2 is recruited to these junctions (Yu et al., 1999) and injection of either APC2 or EB1 dsRNA results in a loss of polarization (Lu et al., 2001). In this study, we have shown that spindle orientation in postcellularized mitotic domains is controlled by Akt activity; spindles in *akt* embryos do not consistently orient parallel to the cortex and the cortical localization of APC2 is disrupted (as in syncytial divisions). These results are consistent with the model proposed in Fig. 10 and suggest that Akt may normally regulate the interaction between APC2, EB1, and the cortex during cellular mitoses, facilitating stable interactions between cortical adherens junctions and MTs.

Work in other systems also suggests a more wide-ranging role for Akt signaling in regulating cell polarity. For example, the reorganization of the MT cytoskeleton associated with mammalian interphase polarized cells has been shown to be dependent on both PI3-K signaling and GSK-3. Inactivation of GSK-3 in this context results in the accumulation of APC at the plus end of MTs associated with the leading edge and reorientation of centrosomes (Nathke et al., 1996; Zumbrunn et al., 2001; Etienne-Manneville and Hall 2003; Fukata et al., 2003). In addition, a recent study has shown that the Akt pathway plays a pivotal role in the stabilization of MTs at the leading cortex of wound-edge cells and that inhibition of GSK-3 affects this stabilization (Onishi et al., 2007). Furthermore, phosphoinositide(3,4,5)P_3, an intermediate of PI3-K signaling, has been shown to organize the basolateral plasma membrane in polarized epithelial cells. Crucially, this accumulation coincides with Akt recruitment to the polarized membrane (Gassama-Diagne et al., 2006). It will therefore be interesting to investigate whether *D. melanogaster* Akt has a role in maintaining stable interactions between MTs and the cortex in cell and developmental contexts other than those described in this study.

Materials and methods

Fly stocks and immunohistochemistry

To verify that the sterility associated with *akt* flies was caused by a loss of Akt activity, we generated $akt1^{04426}/akt1^{q}$ transheterozygote flies. akt^{1q} flies

Downloaded from www.jcb.org on February 15, 2008

(a gift from C. Wilson, University of Oxford, Oxford, UK) possess a point mutation in the ATP-binding domain of the kinase, leading to a non-functional protein (Staveley et al., 1998). Embryos laid by *akt1*^{04426}/*akt1*^{q} transheterozygotes displayed all the phenotypes associated with *akt* embryos. The *sgg*^{1} mutation is the result of an inversion within the transcriptional unit and is effectively a null allele in the early embryo (Ruel et al., 1993). *apc2*$^{\Delta s}$ is a homozygous viable, temperature-sensitive, maternal-effect lethal mutation (McCartney et al., 1999). Stocks were maintained and constructed at 18°C. All analysis was performed at 25°C. Embryos were collected and fixed in methanol (Gergely et al., 2000) with the following exceptions: for APC2 staining, embryos were fixed in 37% formaldehyde (McCartney et al., 1999); for phalloidin, embryos were fixed in 37% formaldehyde before manually devitellinizing. Embryos were blocked for 30 min in PBS, 0.05% Triton X-100, and 3% BSA before incubation overnight in primary antibodies. Antibodies used were: anti–α-tubulin DM1A (1:500; Sigma-Aldrich); anti–γ-tubulin (1:500; Sigma-Aldrich); anti-DHC (1:200; a gift from S. Bullock, University of Cambridge, Cambridge, UK); anti-E-APC (APC2; 1:500; a gift from M. Bienz, University of Cambridge); anti-EB1 (1:500; a gift from R. Vale, Howard Hughes Medical Institute, Chevy Chase, MD), anti-EB1 (1:500; a gift from H. Ohkura, University of Edinburgh, Edinburgh, UK). DNA was visualized with propidium iodide (Sigma-Aldrich; Gergely et al., 2000) and actin with Alexa 633 phalloidin (1:100; Invitrogen). Images were acquired under immersion oil at 25°C using a scanning laser confocal microscope (Radiance Plus; Bio-Rad Laboratories) with a Plan Fluor 40× 1.30 NA H WD0.2 lens (Nikon) and Lasersharp 2000 software (Carl Zeiss, Inc.). Images were converted to JPEG files, pseudocolored, and merged in Photoshop CS2 (Adobe). Levels of Individual channels were adjusted where applicable to maximize pixel range.

Antibody production, immunoprecipitation, and Western blotting

Antiphospho Zw3 antibodies were raised in rabbits by Eurogentec against the phosphopeptide GRPRTSS*FAEGNK (asterisk denotes phosphorylated residue). Affinity-purified antibodies recognized one clear band at 55 kD, which disappeared upon phosphatase treatment (Fig. S1 and not depicted). Flies and dechorionated embryos were frozen in liquid nitrogen before being homogenized and subjected to SDS-PAGE and Western blotting. For anti-Arm immunoprecipitations, 300 wild-type or *akt* embryos were homogenized in 400 μl of C buffer (50 mM Hepes, pH 7.4, 50 mM KCl, 1 mM EGTA, 1 mM PMSF, and 1 mM of protease inhibitors). Extracts were clarified at 14,000 rpm for 10 min before incubation with 20 μl of protein A–Sepharose beads and 50 μl of anti-Arm antibody at 4°C for 2 h. Beads were washed three times with C buffer before being resuspended in 20 μl of 1× protein sample buffer and subjected to SDS-PAGE and Western blotting. Blotted membranes were probed with: antiphospho-Zw3 (1:200), anti-Akt (1:1,000; Cell Signaling Technology), antiphospho(Ser505)-Akt (1:1,000; Cell Signaling Technology), anti-Arm (1:100; Developmental Studies Hybridoma Bank), anti–α-tubulin (1:1,000; Sigma-Aldrich), anti-Zw3 (1:20; a gift from M. Bourouis, Universite de Nice Sophia Antipolis, Nice, France), anti Pros-35 (1:1,000; a gift from P.M. Kloetzel, Humboldt-Universität, Berlin, Germany), and anti-E-APC (APC2; 1:1,000).

Live imaging and quantitative image analysis

Flies expressing GFP-histone and α-tubulin–GFP were obtained from the Bloomington Stock Center and crossed into an *akt1*^{04426}/*akt1*^{q} mutant or *apc2*$^{\Delta S}$ mutant background. Embryos were collected for 1 h and prepared for visualization (Huang and Raff, 1999). Antibody injection experiments were performed essentially as described previously (Gergely et al., 2000). Affinity-purified rabbit anti-Akt antibodies were provided at ∼0.2 mg/ml in Hepes, pH 7.5, and 0.1 mg/ml BSA (Cell Signaling Technology). The antibody–BSA solution was dialyzed into injection buffer (0.1 M Hepes, pH 7.4, and 50 mM KCl), labeled with Alexa 555 according to the manufacturer's instructions (Invitrogen), purified away from an unincorporated label, and concentrated to ∼1 mg/ml anti-Akt and 0.5 mg/ml BSA in a centricon-30 (Millipore). As a control, embryos were injected with 0.5–1.5 mg/ml BSA and labeled with Alexa 555. 1–2-h-old embryos were manually dechorionated on double-sided tape, placed on heptane/glue strips, and allowed to desiccate for 10–12 min before covering with halocarbon oil (Sigma-Aldrich). Embryos were then injected with either labeled anti-Akt or BSA and immediately observed under the confocal microscope. The site of injection was determined using the area of greatest Alexa 555 intensity and the surrounding region was selected for time-course imaging. All images of histone-GFP and tubulin-GFP were collected once every 10 s using a laser scanning confocal microscope (Radiance 2000; Bio-Rad Laboratories). All images represent single focal planes. Videos were exported as BMP files and processed using purpose designed automated tracking software. The automated centrosome/MT tracking software is based on the application of a Fast Level Sets algorithm to define areas of interest. This method has previously been described for the tracking of chromosome dynamics in early *D. melanogaster* embryos (Yau and Wakefield, 2007). The centrosome tracking application allows the user to designate individual nuclei and associated centrosomes and calculates both the angle of centrosomal pair separation and the distance around the defined nuclear envelope from the center of each of the defined centrosomes. This process is automatically repeated for subsequent frames. Data were exported into Excel (Microsoft) and converted from pixel to micrometer values using graticule measurements obtained under the confocal microscope. The angle of centrosome separation just before NEB was calculated automatically by defining the center of the nucleus and the center of the two centrosomes 20 s (2 frames) before NEB. Data were acquired from 100 randomly selected nuclei from five wild-type and *akt* embryos. Centrosome tracking data over time was acquired from 26 wild-type nuclei (from four different embryos), and 16 *akt* nuclei (from three different embryos).

Online supplemental material

Fig. S1 A shows an example of a 2–4-h-old *akt1*^{04226} embryo classified as "other" within Table I. Fig. S1 B shows a full-length Western blot of the affinity-purified antiphospho-Zw3 antibody. Fig. S2 shows individual frames from control- and anti-Akt–injected embryos expressing α-tubulin–GFP. Video1 shows a syncytial embryo expressing Akt-tGFP. Videos 2 and 3 show wild-type and *akt1*^{04426}/*akt1*^{q} syncytial embryos, respectively, expressing histone H2B-GFP. Videos 4–8 show syncytial embryos expressing α-tubulin–GFP. Video 4 shows wild-type embryos, Video 5 shows *akt* mutant embryos, Video 6 shows embryos injected with anti-Akt antibodies, and Video 7 shows a control-injected embryo. Video 8 shows apc2$^{\Delta s}$ embryos. Videos 9 and 10 show *akt* mutant (Video 1) and anti-Akt injected (Video 2) syncytial embryos expressing α-tubulin–GFP. Online supplemental material is available at available at http://www.jcb.org/cgi/content/full/jcb.200705085/DC1).

We thank Katherine Fisher and Shan Gao for their critical reading of the manuscript. We thank Robin Freeman for advice and assistance with the centrosome tracking software. We thank Hiro Ohkura, Ron Vale, Marc Bourouis, Simon Bullock, Marianne Bienz, Peter Koetzel, and Clive Wilson for providing antibodies and flies.

J.G. Wakefield is funded through a lectureship associated with the Engineering and Physical Sciences Research Council (EPSRC) Oxford Life Sciences Interface Doctoral Training Centre. Support for G.J. Buttrick was provided by the Medical Research Council; L.M.A. Beaumont and C. Yau are funded by the EPSRC Oxford Life Sciences Interface Doctoral Training Centre; and J.R. Hughes was funded by the Biotechnology and Biological Sciences Research Council (grant BBS/B/08019).

Submitted: 15 May 2007
Accepted: 7 January 2008

References

Allan, V., and I.S. Nathke. 2001. Catch and pull a microtubule: getting a grasp on the cortex. *Nat. Cell Biol.* 3:E226–E228.

Andjelkovic, M., D.R. Alessi, R. Meier, A. Fernandez, N.J. Lamb, M. Frech, P. Cron, P. Cohen, J.M. Lucocq, and B.A. Hemmings. 1997. Role of translocation in the activation and function of protein kinase B. *J. Biol. Chem.* 272:31515–31524.

Berrueta, L., J.S. Tirnauer, S.C. Schuyler, D. Pellman, and B.E. Bierer. 1999. The APC-associated protein EB1 associates with components of the dynactin complex and cytoplasmic dynein intermediate chain. *Curr. Biol.* 9:425–428.

Brunet, A., A. Bonni, M.J. Zigmond, M.Z. Lin, P. Juo, L.S. Hu, M.J. Anderson, K.C. Arden, J. Blenis, and M.E. Greenberg. 1999. Akt promotes cell survival by phosphorylating and inhibiting a Forkhead transcription factor. *Cell.* 96:857–868.

Cliffe, A., J. Mieszczanek, and M. Bienz. 2004. Intracellular shuttling of a *Drosophila* APC tumour suppressor homolog. *BMC Cell Biol.* 5:37.

Coffer, P.J., J. Jin, and J.R. Woodgett. 1998. Protein kinase B (c-Akt): a multifunctional mediator of phosphatidylinositol 3-kinase activation. *Biochem. J.* 335:1–13.

Cong, L.N., H. Chen, Y. Li, L. Zhou, M.A. McGibbon, S.I. Taylor, and M.J. Quon. 1997. Physiological role of Akt in insulin-stimulated translocation of GLUT4 in transfected rat adipose cells. *Mol. Endocrinol.* 11:1881–1890.

Cross, D.A., D.R. Alessi, P. Cohen, M. Andjelkovich, and B.A. Hemmings. 1995. Inhibition of glycogen synthase kinase-3 by insulin mediated by protein kinase B. *Nature.* 378:785–789.

Downloaded from www.jcb.org on February 15, 2008

Cross, D.A., P.W. Watt, M. Shaw, J. van der Kaay, C.P. Downes, J.C. Holder, and P. Cohen. 1997. Insulin activates protein kinase B, inhibits glycogen synthase kinase-3 and activates glycogen synthase by rapamycin-insensitive pathways in skeletal muscle and adipose tissue. *FEBS Lett.* 406:211–215.

Cytrynbaum, E.N., J.M. Scholey, and A. Mogilner. 2003. A force balance model of early spindle pole separation in *Drosophila* embryos. *Biophys. J.* 84:757–769.

Cytrynbaum, E.N., P. Sommi, I. Brust-Mascher, J.M. Scholey, and A. Mogilner. 2005. Early spindle assembly in *Drosophila* embryos: role of a force balance involving cytoskeletal dynamics and nuclear mechanics. *Mol. Biol. Cell.* 16:4967–4981.

Dan, H.C., M. Sun, L. Yang, R.I. Feldman, X.M. Sui, C.C. Ou, M. Nellist, R.S. Yeung, D.J. Halley, S.V. Nicosia, et al. 2002. Phosphatidylinositol 3-kinase/Akt pathway regulates tuberous sclerosis tumor suppressor complex by phosphorylation of tuberin. *J. Biol. Chem.* 277:35364–35370.

Etienne-Manneville, S., and A. Hall. 2003. Cdc42 regulates GSK-3beta and adenomatous polyposis coli to control cell polarity. *Nature.* 421:753–756.

Foe, V.E. 1989. Mitotic domains reveal early commitment of cells in *Drosophila* embryos. *Development.* 107:1–22.

Frenz, L.M., and D.M. Glover. 1996. A maternal requirement for glutamine synthetase I for the mitotic cycles of syncytial *Drosophila* embryos. *J. Cell Sci.* 109:2649–2660.

Fukata, M., M. Nakagawa, and K. Kaibuchi. 2003. Roles of Rho-family GTPases in cell polarisation and directional migration. *Curr. Opin. Cell Biol.* 15:590–597.

Gassama-Diagne, A., W. Yu, M. ter Beest, F. Martin-Belmonte, A. Kierbel, J. Engel, and K. Mostov. 2006. Phosphatidylinositol-3,4,5-trisphosphate regulates the formation of the basolateral plasma membrane in epithelial cells. *Nat. Cell Biol.* 8:963–970.

Gergely, F., D. Kidd, K. Jeffers, J.G. Wakefield, and J.W. Raff. 2000. D-TACC: a novel centrosomal protein required for normal spindle function in the early *Drosophila* embryo. *EMBO J.* 19:241–252.

Goode, B.L., D.G. Drubin, and G. Barnes. 2000. Functional cooperation between the microtubule and actin cytoskeletons. *Curr. Opin. Cell Biol.* 12:63–71.

Green, R.A., R. Wollman, and K.B. Kaplan. 2005. APC and EB1 function together in mitosis to regulate spindle dynamics and chromosome alignment. *Mol. Biol. Cell.* 16:4609–4622.

Huang, J., and J.W. Raff. 1999. The disappearance of cyclin B at the end of mitosis is regulated spatially in *Drosophila* cells. *EMBO J.* 18:2184–2195.

Lu, B., F. Roegiers, L.Y. Jan, and Y.N. Jan. 2001. Adherens junctions inhibit asymmetric division in the *Drosophila* epithelium. *Nature.* 409:522–525.

McCartney, B.M., H.A. Dierick, C. Kirkpatrick, M.M. Moline, A. Baas, M. Peifer, and A. Bejsovec. 1999. *Drosophila* APC2 is a cytoskeletally-associated protein that regulates wingless signaling in the embryonic epidermis. *J. Cell Biol.* 146:1303–1318.

McCartney, B.M., D.G. McEwen, E. Grevengoed, P. Maddox, A. Bejsovec, and M. Peifer. 2001. *Drosophila* APC2 and Armadillo participate in tethering mitotic spindles to cortical actin. *Nat. Cell Biol.* 3:933–938.

Nathke, I.S., C.L. Adams, P. Polakis, J.H. Sellin, and W.J. Nelson. 1996. The adenomatous polyposis coli tumor suppressor protein localizes to plasma membrane sites involved in active cell migration. *J. Cell Biol.* 134:165–179.

Onishi, K., M. Higuchi, T. Asakura, N. Masuyama, and Y. Gotoh. 2007. The PI3K-Akt pathway promotes microtubule stabilisation in migrating fibroblasts. *Genes Cells.* 12:535–546.

Papadopoulou, D., M.W. Bianchi, and M. Bourouis. 2004. Functional studies of shaggy/glycogen synthase kinase 3 phosphorylation sites in *Drosophila melanogaster*. *Mol. Cell. Biol.* 24:4909–4919.

Peifer, M., and P. Polakis. 2000. Wnt signaling in oncogenesis and embryogenesis–a look outside the nucleus. *Science.* 287:1606–1609.

Robinson, J.T., E.J. Wojcik, M.A. Sanders, M. McGrail, and T.S. Hays. 1999. Cytoplasmic dynein is required for the nuclear attachment and migration of centrosomes during mitosis in *Drosophila*. *J. Cell Biol.* 146:597–608.

Rogers, S.L., G.C. Rogers, D.J. Sharp, and R.D. Vale. 2002. *Drosophila* EB1 is important for proper assembly, dynamics, and positioning of the mitotic spindle. *J. Cell Biol.* 158:873–884.

Rothwell, W.F., P. Fogarty, C.M. Field, and W. Sullivan. 1998. Nuclear-fallout, a *Drosophila* protein that cycles from the cytoplasm to the centrosomes, regulates cortical microfilament organization. *Development.* 125:1295–1303.

Ruel, L., V. Pantesco, Y. Lutz, P. Simpson, and M. Bourouis. 1993. Functional significance of a family of protein kinases encoded at the shaggy locus in *Drosophila*. *EMBO J.* 12:1657–1669.

Sharp, D.J., H.M. Brown, M. Kwon, G.C. Rogers, G. Holland, and J.M. Scholey. 2000. Functional coordination of three mitotic motors in *Drosophila* embryos. *Mol. Biol. Cell.* 11:241–253.

Shaw, M., P. Cohen, and D.R. Alessi. 1997. Further evidence that the inhibition of glycogen synthase kinase-3beta by IGF-1 is mediated by PDK1/PKB-induced phosphorylation of Ser-9 and not by dephosphorylation of Tyr-216. *FEBS Lett.* 416:307–311.

Shtivelman, E., J. Sussman, and D. Stokoe. 2002. A role for PI 3-kinase and PKB activity in the G2/M phase of the cell cycle. *Curr. Biol.* 12:919–924.

Siegrist, S.E., and C.Q. Doe. 2007. Microtubule-induced cell polarity. *Genes Dev.* 21:483–496.

Spradling, A.C., D. Stern, A. Beaton, E.J. Rhem, T. Laverty, N. Mozden, S. Misra, and G.M. Rubin. 1999. The Berkeley Drosophila Genome Project gene disruption project: Single P-element insertions mutating 25% of vital *Drosophila* genes. *Genetics.* 153:135–177.

Staveley, B.E., L. Ruel, J. Jin, V. Stambolic, F.G. Mastronardi, P. Heitzler, J.R. Woodgett, and A.S. Manoukian. 1998. Genetic analysis of protein kinase B (AKT) in *Drosophila*. *Curr. Biol.* 8:599–602.

Stevenson, V.A., J. Kramer, J. Kuhn, and W.E. Theurkauf. 2001. Centrosomes and the Scrambled protein coordinate microtubule-independent actin reorganization. *Nat. Cell Biol.* 3:68–75.

Su, L.K., M. Burrell, D.E. Hill, J. Gyuris, R. Brent, R. Wiltshire, J. Trent, B. Vogelstein, and K.W. Kinzler. 1995. APC binds to the novel protein EB1. *Cancer Res.* 55:2972–2977.

Sullivan, W., and W.E. Theurkauf. 1995. The cytoskeleton and morphogenesis of the early *Drosophila* embryo. *Curr. Opin. Cell Biol.* 7:18–22.

Sullivan, W., P. Fogarty, and W. Theurkauf. 1993. Mutations affecting the cytoskeletal organization of syncytial *Drosophila* embryos. *Development.* 118:1245–1254.

Townsley, F.M., and M. Bienz. 2000. Actin-dependent membrane association of a *Drosophila* epithelial APC protein and its effect on junctional Armadillo. *Curr. Biol.* 10:1339–1348.

Wakefield, J.G., D.J. Stephens, and J.M. Tavare. 2003. A role for glycogen synthase kinase-3 in mitotic spindle dynamics and chromosome alignment. *J. Cell Sci.* 116:637–646.

Yamashita, Y.M., D.L. Jones, and M.T. Fuller. 2003. Orientation of asymmetric stem cell division by the APC tumor suppressor and centrosome. *Science.* 301:1547–1550.

Yau, C., and J. Wakefield. 2007. Quantitative image analysis of chromosome dynamics in early *Drosophila* embryos. *In* Biomedical Imaging: From Nano to Macro, 2007. ISBI 2007. 4th IEEE International Symposium on. IEEE, Arlington, VA. 264–267.

Yu, X., L. Waltzer, and M. Bienz. 1999. A new *Drosophila* APC homologue associated with adhesive zones of epithelial cells. *Nat. Cell Biol.* 1:144–151.

Zhou, F.Q., J. Zhou, S. Dedhar, Y.H. Wu, and W.D. Snider. 2004. NGF-induced axon growth is mediated by localized inactivation of GSK-3beta and functions of the microtubule plus end binding protein APC. *Neuron.* 42:897–912.

Zumbrunn, J., K. Kinoshita, A.A. Hyman, and I.S. Nathke. 2001. Binding of the adenomatous polyposis coli protein to microtubules increases microtubule stability and is regulated by GSK3 beta phosphorylation. *Curr. Biol.* 11:44–49.

Downloaded from www.jcb.org on February 15, 2008